TD-DFT study of small organic molecules based on Boron subphthalocyanines by modifying axial substituents for organic photovoltaics

Faheem Abbas[1], Tayyaba Nasir[1], Muhammad Awais Ahmad[3], Saira Sehar[2], Rida Zulfiqar[1], Muhammad Shaid Iqbal[3], Muhammad Ishaq[1]

[1]University of Agriculture Faisalabad, Pakistan
[2]Minhaj University Lahore, Pakistan
[3]Government College University Faisalabad, Pakistan

DOI: 10.29322/IJSRP.11.03.2021.p11151
http://dx.doi.org/10.29322/IJSRP.11.03.2021.p11151

Graphical Abstract

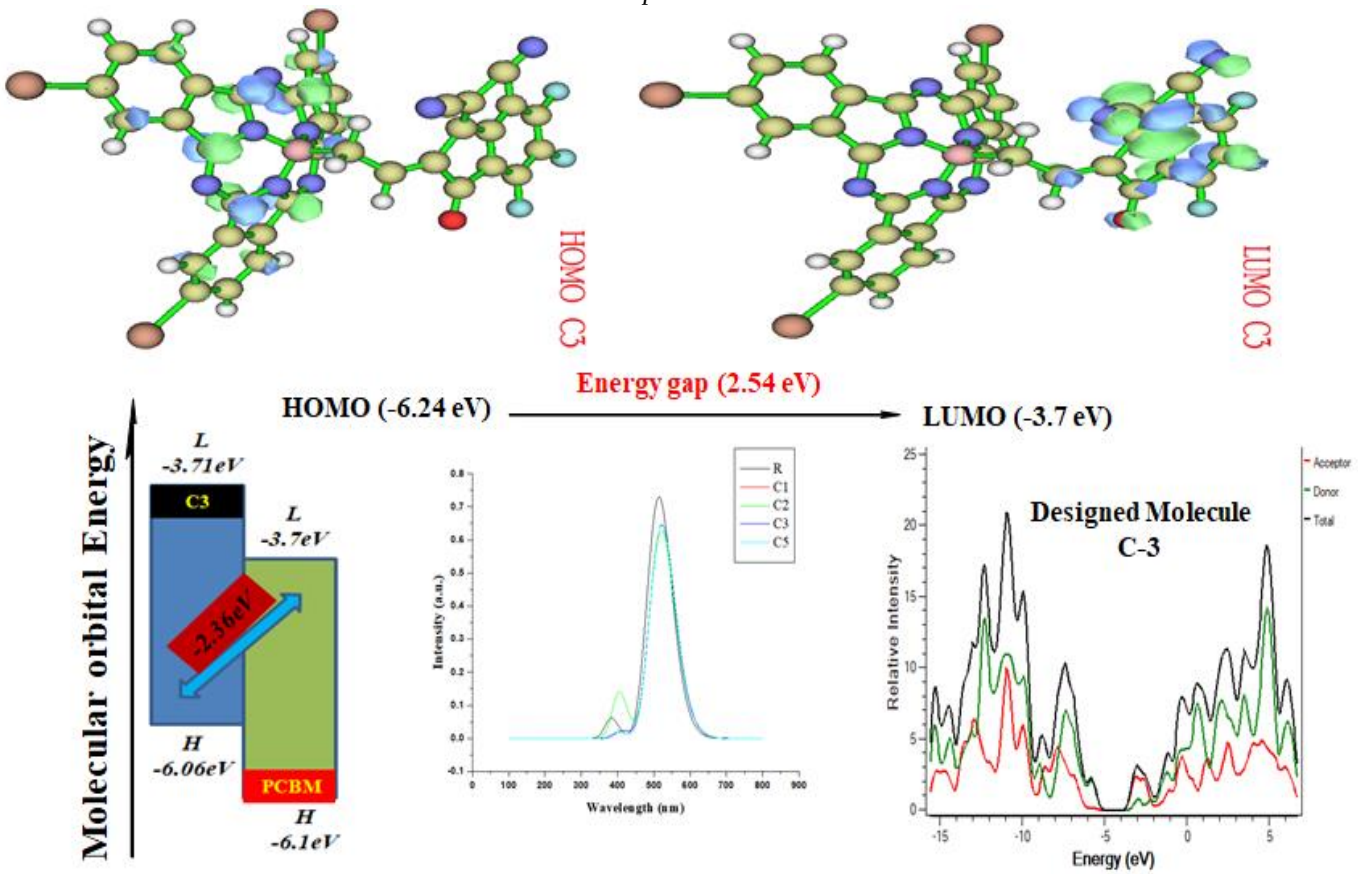

ABSTRACT

To boost the performance of solar cells (SCs), four non-fullerene π-conjugated acceptor compounds, including iodo-substituted (SubPcs) subphthalocyanines is π-conjugated rigid tetrahedral geometry aromatic molecule composed of three units combined around a boron atom bearing a macrocycle core with a perpendicular axial ligand. The **C3** designed molecule shows the optoelectronic analysis is better than the reference molecule **R** due to absorption range because its range found to be nearer the reference compound as well as the absorption occur at 645.53 nm, 519 nm respectively. Examination of the frontier molecular orbital

(FMO) as well as transition density matrix (TDM) are performed that offers fundamental knowledge on the distribution of charges and electronic excitation, as well as the process of transition between the examined compound. The overall reported molecules show the charge density which is spread over the whole molecules. With a small band difference of 2.54 eV, the **C3** compound effectively move their electron density from the maximum or higher energy state named as (HOMO) to the lowest energy state such as (LUMO). It has been shown that the structural tailoring of the terminal will efficiently modify the frontier molecular orbital such as HOMO and LUMO, captivation spectra, energy band difference, and open-circuit voltage and reorganization energy of the compounds under investigation. Our findings indicate that the compounds under examination acted as fine-donating materials. In addition, a few of the compounds under examination may be used as a hole as well as transport of electrons material for OSC.

Introduction

The mostly used modern sources of energy used worldwide include water, petroleum storage products and coal even these sources may have a lot of threats around the world environment. These energy sources are depleting day by day due to over usage [1]. So due to this reason, alternative to these sources, it's the need of time to discover more sources of energy which should be environmentally friendly and also have renewable feature. Photovoltaic devices are the most efficient cells in this regard as they contain remarkable properties like solution processibility. A huge amount of energy can be produced through photovoltaic devices [2].Organic photovoltaics are polymer composed substances having less expensive nature. Organic photovoltaic solar devices contain remarkable optical and electronic characteristics [3].The interest of research on photovoltaics have been strengthening as the awareness of sources of fossil energy grown rapidly since last decade worldwide. These are consistent and long term available materials known now a days [4].

Solar energy, fuel cells are most promising energy creating technology for the production of renewable energy [1]. High power conversion efficiency of up to 44.4% has been achieved from inorganic solar cells like silicon solar cells[2]. Inorganic solar cells have some drawbacks in terms of costly content, are not environmentally friendly, and exhibit complex behavior during fabrication [4].Organic solar cells proved to be a promising candidate for converting solar energy compared to inorganic solar cells due to their lightweight and low cost[5]. Nowadays, solution-processable bulk heterojunction (BHJ) solar cells has been dominated in OPV cells with a PCE of up to 12%[6].

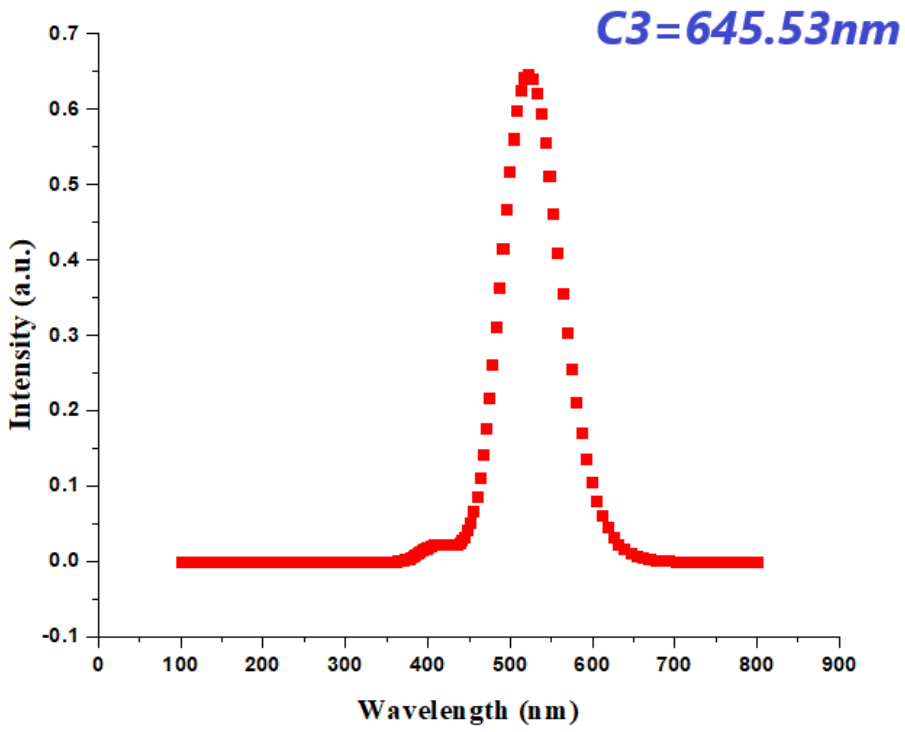

Fig:1 Absorption spectra of newly designed molecule **C3**

In OSCs, fullerene and its derivatives are widely used electron receptors nowadays e.g. [6, 6]-phenyl-C61-butyricacid-methyl-ester (PC61BM), PC71BM, indene C60 bis adduct IC60BA and IC70BA etc are also used due to rapid electron mobility and nanoscale transformation of PM-OSC D-A molecules(Cheng et al., 2014). Research on non-fullerene receptors (NFAs) has progressed rapidly in recent years and has resulting in outstanding performance of OSCs with PCE of up to 17%[8]. Device performance dependent on terminal groups and spacers. Very low band approximately. 1, 65 eV polymer molecule (3-hexyl-2,5-thienylene vinylene) was synthesized using acyclic diene polymerization and implemented in BHJ-SCs with PCBM. Almost 60 % of the maximum performance of PM-SCs was found from PCBM thin film with polymer, and higher PCEs were also observed. [9].

In the last few years, more than 9% power conversion efficiency (PCEs) has been recorded for OPVs focused on conjugated polymers as electron donor materials. Among the numerous small molecules developed for solution-processed solar cells, molecules including benzo-[1,2-b:4,5-b0] dithiophen (BDT) building blocks have emerged with good OPV efficiency. BDT, for the following purposes, was chosen as an appealing donor building block for donor molecules in OPVs. Firstly, its structural symmetry and the rigid fused aromatic system could improve the delocalization of electrons and enable solid state cofacial p-p stacking, while benefting the devices' charge transport. BDT will stabilize the energy density of the resulting molecules at the lowest occupied molecular orbital (HOMO)[1].

Recently PCE of SubPcs was obtained over 8% due to attachment of dialkylthiol substituted BDT homopolymer. In BDT molecule the acceptor fragment contains sulphur, oxygen and nitrogen due to these atoms the acceptor gave good efficiency, and also gave effectiveness in results and due to this acceptor groups, the ICT is also improved. To enhance the photovoltaic performance two different alkyl chains, 2-ethylhexyl and 2-hexyldecyl were employed on the thiophene unit. So overall it is very good acceptor but to improve the more efficiency we designed four other molecules namely; **C1**, **C2**, **C3** and **C4**. The designed molecule is formed by the replacement of acceptor group. The optical and electronic properties of developed molecules were then compared with the reference molecule **R.**

Computational Details

For the geometry optimization and electronic properties of newly developed molecules, the distribution patterns of frontier molecular Orbitals (FMOS) are considered. All the calculations were carried out on the Gaussian 09[16]. The density functional theory was implemented to optimize all molecules' geometry with anion, cation, and neutral density[17]. By using CAM-B3LYP [18], MPW1PW91 [19], B3LYP [20], and WB97XD [21]theory stage, and 6-31 G(d, p) [22] theory level at basis set. Using the four different functionals hybrid for the ground state's geometry optimization for the reference molecule R, MPW1PW91, B3LYP, WB97XD, and CAM-B3LYP optimized by using the basis set 6-31G, at (d, p) level [23].TD-SCF was employed for the electronic and excited-state calculations joined with absorption spectra, usually used for up to 100 atoms[24].

For absorption spectra, toluene was used as an isotropic solvent taken from the IEFPCM [25]. After optimizing the reference molecule with different hybrid functional, λmax was then compared with the experimental value found in the literature. For the visualization of absorption spectra, Wizard software was used through Origin 6.0[26].

For geometrically designed structures, the molecules' reorganization energies have been determined at the B3LYP / Lan2D G (d, p).slevel. The energy of reorganization consists of two components, the strength of external reorganization (λext) and the energy of internal reorganization (λint). The λext represents the influence of distortion on an ambient medium, while λint is a function of rapid molecular structure transition[27]. The estimated external energy values for reorganization were poor in condensed pure organic phases and far lower than their internal components.

$$\lambda_{+=}[E_0^{+}{}_{-}E_{+}] + [E^{0}{}_{+} - E_0] \quad (1)$$

$$\lambda_{-} = [E^{-}{}_{0-}E_{-}] + [E_{-}{}^{0} - E_0] \quad (2)$$

E10 (E20) expresses the energy cation (anion), measured at the neutral molecule's optimized structure. E+ (E-) is also the cation energy (anion) that is predicted through the neutral molecule's optimized cation structure (anion). Additionally, at ground level, E0 reflects that the neutral molecule and E0 + (E0-) energy would be a neutral molecule's energy at optimized cation design (anion). The density of state (DOS) represents an increase in levels of energy per unit of atoms. DOS also describes the semiconductor materials ' electronic form. The state density is also explained at the specific energy level were computed through PyMOlyze with the same basis set[28]. For Wave function analysis, Multiwfn was used for visualizing real space function and transition density matrix files[29].

3. Results and discussions

First of all, **the R** reference molecule was investigated with four different methods like B3LYP, CAM-B3LYP, MPW1PW91, and WB97XD. Their absorption values were 598.53nm, 625.41 nm, 605.09nm, 558.37 respectively.

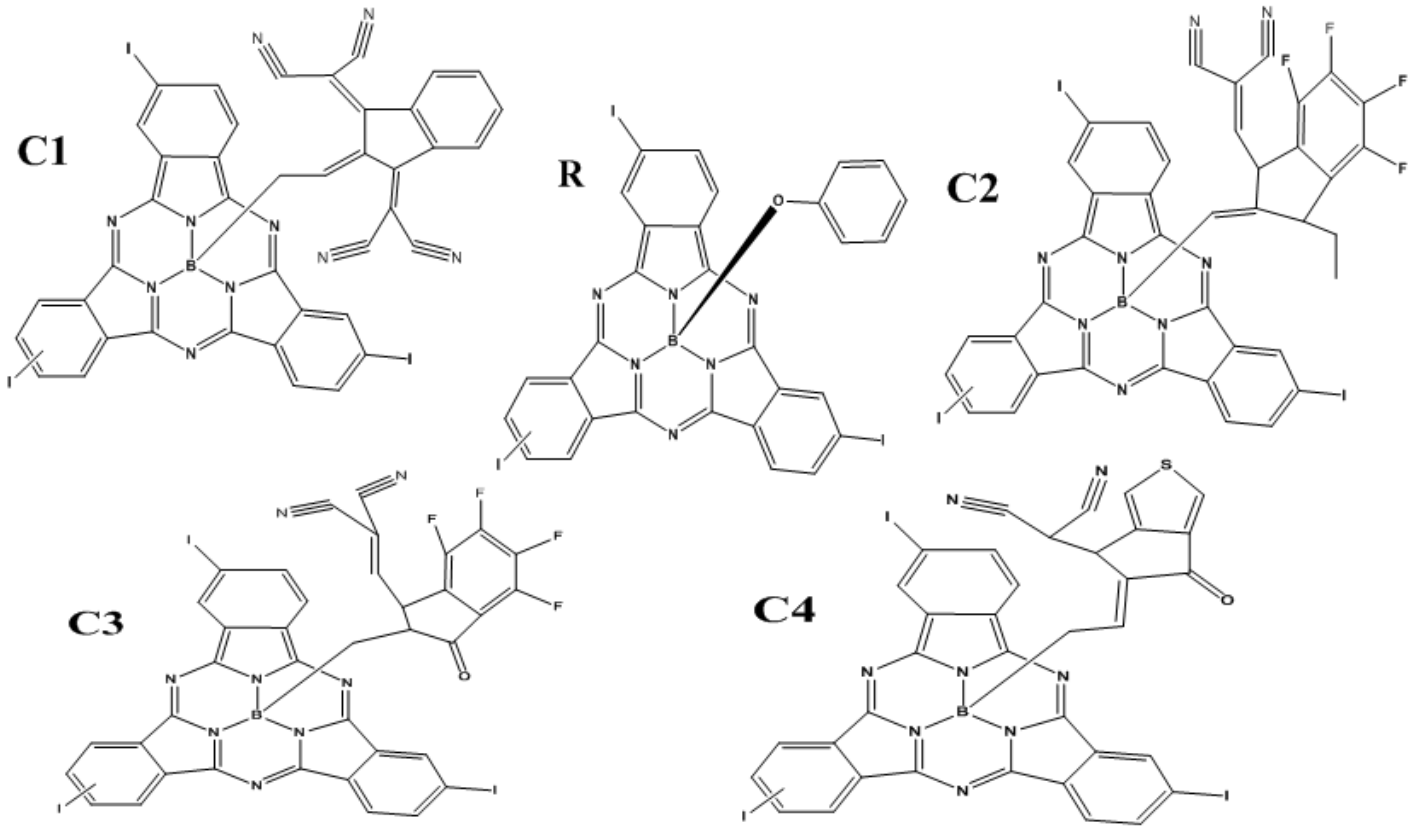

Figure 2. ChemDraw molecular structure of (**R**) reference molecule and a developed donor molecule (**C1**- **C4**)

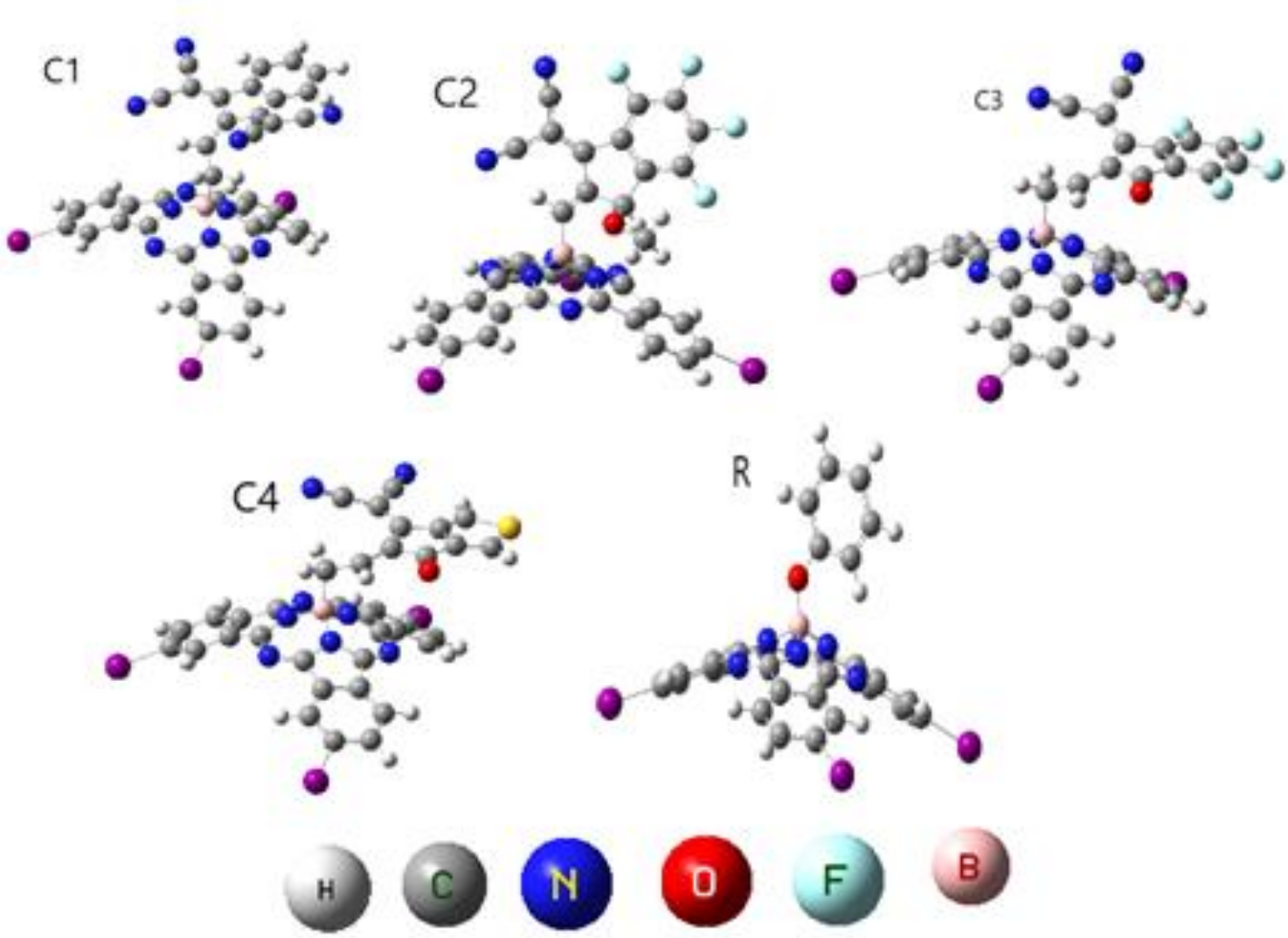

Figure 3. Optimized structure of (**R**) reference molecule and developed donor molecules (**C1-C4**) optimized at ground level the theoretical stage of B3LYP at Lan2DZ (G) d, p with toluene solvent

The MPWIPW91 basis set and hybrid functional 6-31G (G) d, p was selected as best for all further calculations.TD-DFT was used at B3LYP / Lan2D G (d, p).s basis set to calculate the absorption spectra of the newly constructed small molecules (**C1-C4)** and **R** with solvent and without toluene (gas phase).

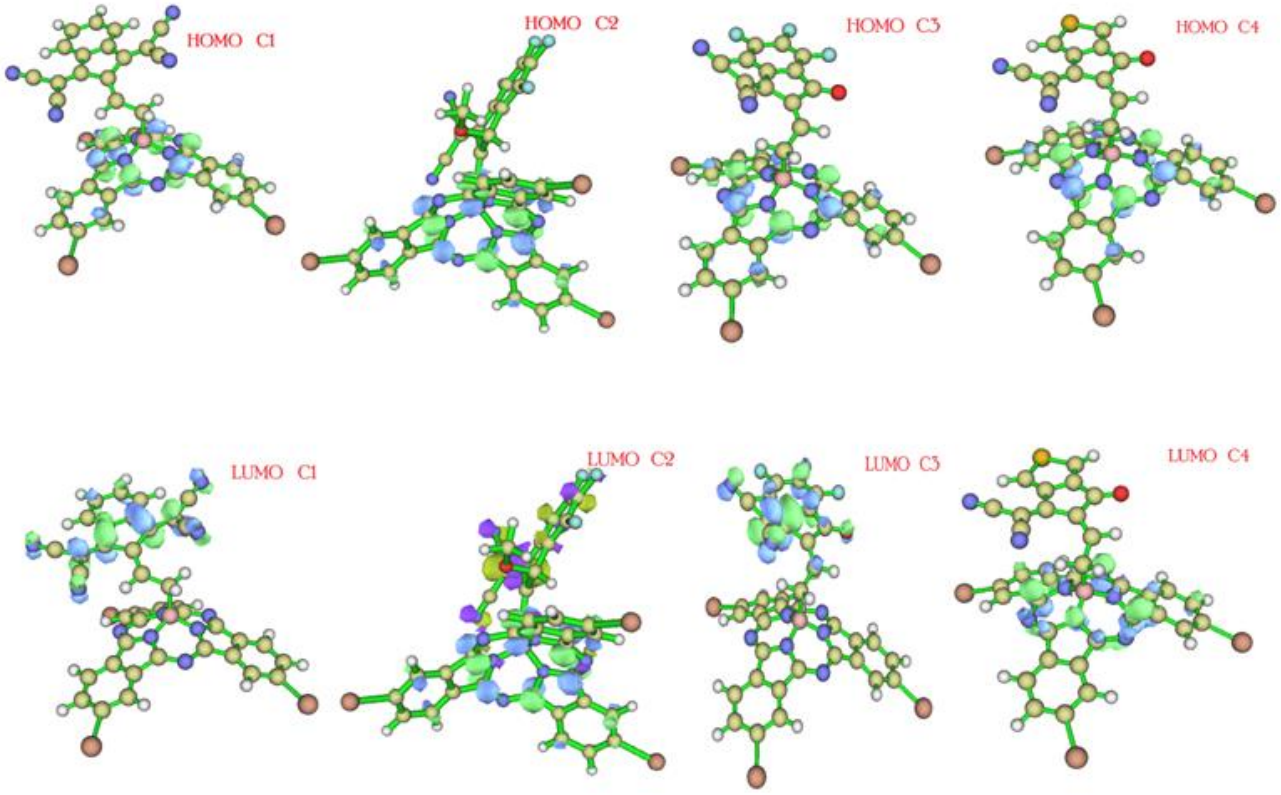

Fig.4. Theoretical structures of molecular frontier orbital distribution for reference molecules(**R**) and developed molecules (**C1-C4**) at B3LYP at Lan2DZ (G) d, p with toluene solvent

Table 1. The energy of HOMO, LUMO and its energy difference B3LYP at Lan2DZ (G) d, p with toluene solvent

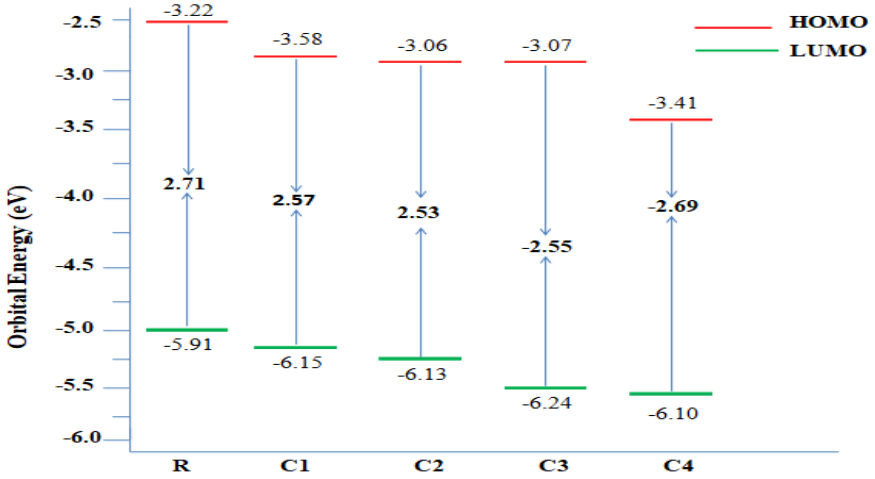

Fig.5. The energy gap of developed molecules C1-C4 and R using Origin 6.0.

Table: 2 Energy gap of all newly developed molecules and reference R

3.1. Quantum Mechanical Approach

Molecular orbital frontier distribution patterns define the electronic and optical characteristics of newly developed molecules. The ability to accept or donate electrons is indicated by the lowest unoccupied orbital (LUMO) around the highest molecular orbit (HOMO), as shown in (Fig4). The recently developed molecules (**C1-C4)** are designed to prevent self-assembly. The newly developed HOMO values for the small molecules (**C1-C4)** are -5.27, -5.49, -5.53, and -5.59 eV, and the LUMO values for **C1** to **C4** are-2.84,-2.86, -2.99, and -3.34 eV, respectively in (Fig 5). The HOMO-LUMO energy gap (Eg) refers to the chemical reactivity of various

Molecules	**E_{HOMO} (eV)**	**E_{LUMO} (eV)**	**Eg (eV)**
R	-5.93	-3.22	2.23
C1	-6.15	-3.58	2.57
C2	-6.13	-3.06	2.53
C3	-6.24	-3.07	2.54
C4	-6.10	-3.41	2.69

substituents. These newly structured small molecules (**C1-C4)** have energy gaps of 2.40eV, 2.50eV, 2.19eV, and 2.25eV. The reference R molecule has an energy gap of 2.19eV, as shown in (Table 1). The critical framework is band gap, and Charge transfer depends on the energy gap. In this research, Eg is within the 2.19-2.50eV range. Basically energy gap is required to move the electron from ground state to excited state. The lowest energy gap of 2.19eV of **C3** is associated with its more stable LUMO due attachment of cyanoacrylate acceptor groups.

Thus, the stronger the conjugation, the greater the electron's transition from HOMO to LUMO due to the smaller Eg.**C3** has lower energy gap than **C4** due to presence of strong electron-withdrawing methylene malononitrile conjugation with thiophene acceptor groups.**C1** molecule exhibited very smaller energy gap than the reference molecule **C2** due to electron acceptor (Z)-5-ethylidene-3-methylthiazolidine-2, 4-dione thiophene end cape group. Different changes in the distribution of electrons in fundamental molecular orbitals have occurred due to the molecules' different nature attached to it by the acceptor. Different types of electron acceptor species modified the distribution pattern of the electrons on the molecular orbitals. These results were further validated for all of these molecules by the state's density involving LUMO and HOMO. The State density also shows the analysis of the distribution pattern. Zero density status states the energy level is not in control. There are five different color types in the state density graph, red, green, blue, black, and pink. The blue and green line indicates the energy level of HOMO, and the energy level of LUMO is shown by the red and the pink line. Varying energies represent band gap in the LUMO and HOMO. So, the difference between the green and the red line is band gap

Electron-withdrawing moties can influence the electron density for all the HOMOs and LUMOs in electronic state density. The energy of molecular orbitals occupied and DOS characterizes unoccupied. The DOS of HOMO is the same for all designed (**C1-C4**), and **R** molecules indicate that HOMO originally comes from the bridge and the donor side. LUMO of all molecules is different due to unoccupied molecular orbitals from the end-capped acceptor moties, and a little bit spreads over the bridge.

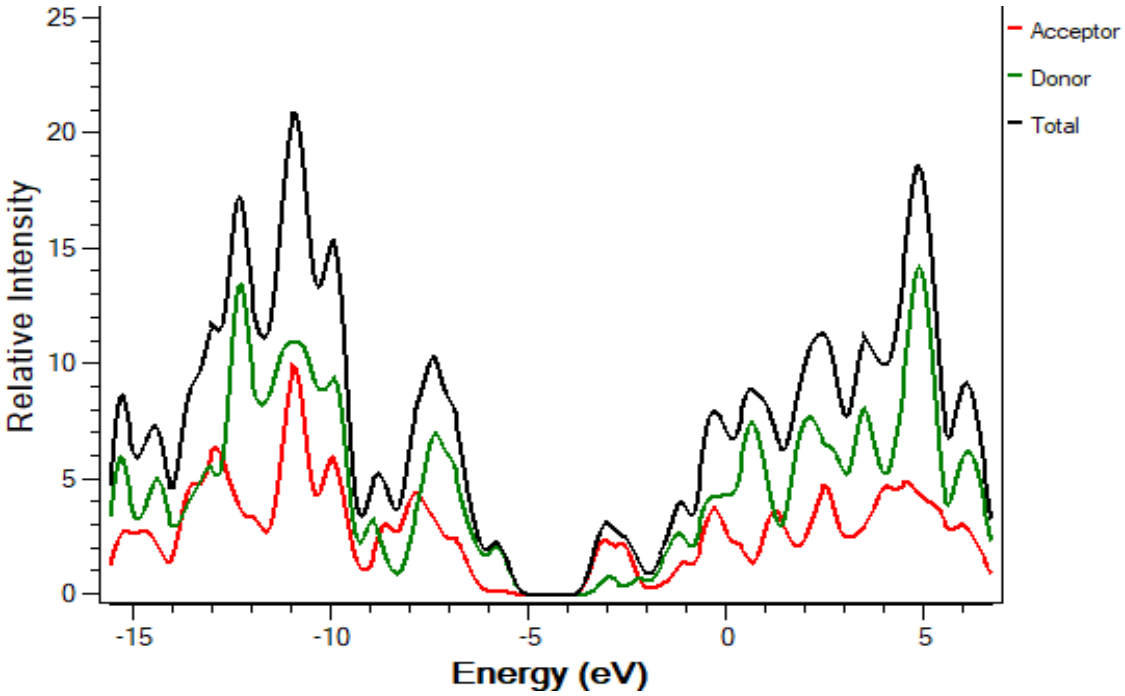

Fig.6. State density of both the newly developed small molecules **C3**, around LUMO as well as HOMO and the basis set 6-31G (d, p) **R** molecule.

3.2. Optical Properties

The absorption spectra were analyzed and measured using TD-DFT. Firstly, **R** was examined through different functionalities such as B3LYP, CAM-B3LYP, MPW1PW91, and WB97XD our absorption values of 598.53 nm, 624.41 nm 645.53 nm, and 558.37nm. MPW1PW91 with basis set 6-31G was selected for further calculations because its λmax (645.53 nm) was close to experimental values found in the literature. The λmax shows reciprocal trend with the Eg values[30]. The larger the λmax value of the compounds, the smaller would be the Eg value. Hence, B3LYP / Lan2D G (d, p).s with basis set 6-31G (d, p). The U.V/ visible spectra of the newly developed small molecules **C1**, **C2**, **C3**, **C4,** and the **R** reference molecule with solvent and without solvent (gas phase) were calculated using TD-DFT at B3LYP / Lan2D G (d, p).s basis. Calculations on the molecules ' initial four transition states were also carried out in the gas phase. Some of the other properties for all molecules, such as dipole moment, were also calculated. Throughout the investigation, we found an inverse relationship between the absorption and energy gap. Band gap energy decreases of designed molecules due to electron-withdrawing acceptor moties are attached to the donor core.

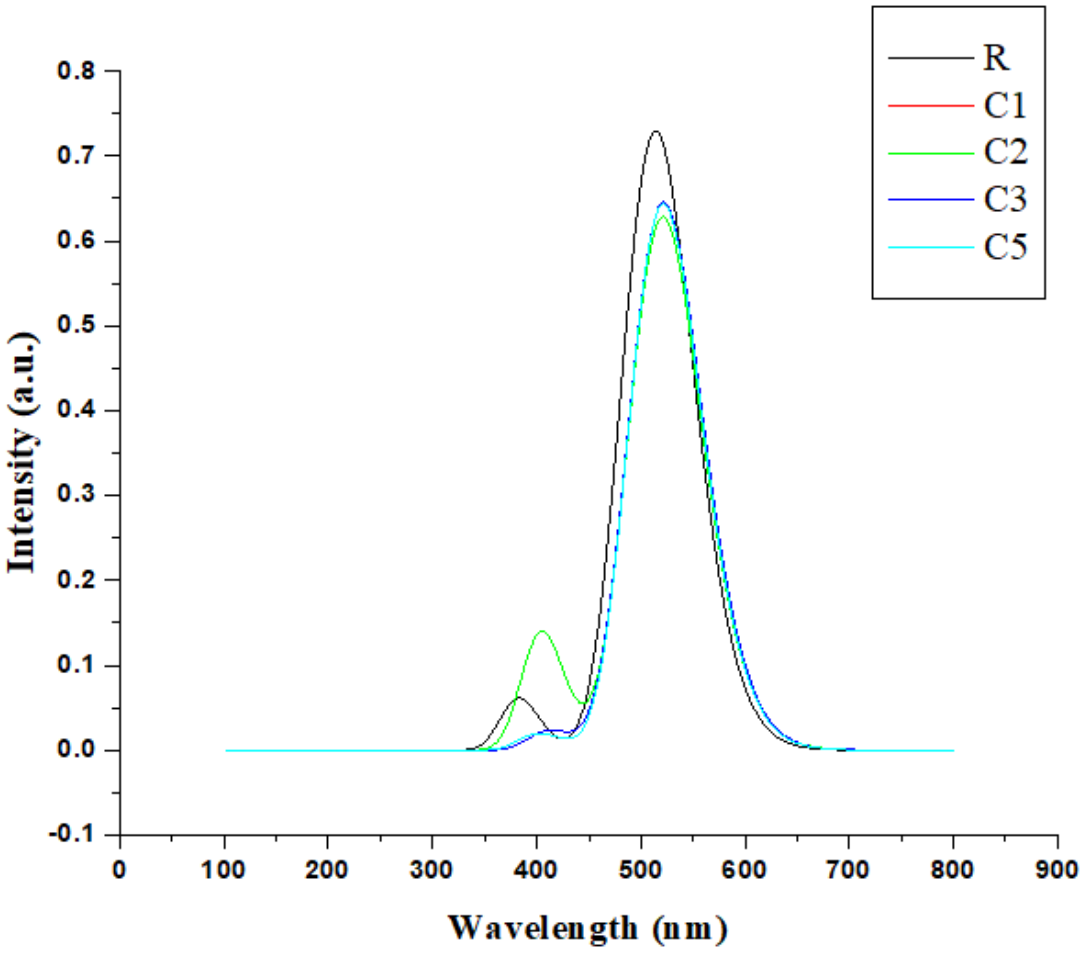

Fig7: The absorption spectra of all designed molecules with reference molecule

The absorption spectra of **C3** are blue shifted 74nm from **R**. When the effect of electron withdrawal moieties on the acceptor then increased, the absorption also increased. Maximum absorption in the gas phase for the specified small molecules is from 645.53 nm to 625.41ynm. Total absorption (λmax) of all newly designed small-donor molecules was 561.97nm, 563.10 nm, 544.78 nm, and 618.42 nm, respectively. The reference molecule **R** presented the 569.04 nm λmax. Due to the extended conjugation of attached moieties, **C3** exhibited maximum absorption between all newly designed small molecules.

The **C3** molecule represents the maximum λmax due to dimethoxyphenyl malononitrile conjugated with thiophene acceptor groups.

Dipole moment was investigated and determined using theMPW1PW91 reference set with 6-31G (d,p) and all the newly developed small molecules. The Solubility of the newly created small molecules in the organic solvents depends on the dipole moment. The manufacture of organic solar cells is strongly effected by the moment of the dipole. If there is a higher dipole moment value, it will be better for manufacturing. Therefore, if the dipole moment is increased in value, the molecules' Solubility also increases in the different types of organic solvents. Because of the increased dipole moment value, the manufacture and processing of organic solar cells became simpler. The results showed that among all the newly developed small molecules, the **R** molecule exhibited the lowest dipole moment, 4.32D, which describes the poor Solubility of **R** in chloroform. Dipole moment has a great influence on the production of donor content in self-assembly film. **C3** shows the highest dipole moment and greater charge transfer rate due to electron-withdrawing groups.

The higher value also increases the fill factor, reduces the combination of charges, and allows for donor-acceptor substituent planning. We also anticipate the dipole's improved moment to lead to higher self-assembly, resulting in a higher level of order at the recipient-acceptor interface, which would lower the recombination value and improve F.F. The moment of excited state, ground condition and the difference between them.

A dimensionless quantity is used to investigate the transition of electrons between the two states by using oscillator strength. It plays a key role in describing the optical characteristics of both atoms and molecules. Oscillator strength almost seems to be unity in the U.V./Vis region of all organic molecules[31]. The oscillator strength should be less than unity for showing the strong absorption in the visible region. Here we see only greater oscillator strength of **C2** our designed molecules (**C1**-**C4**).

1. The excitation energy value **Ex (eV)**, oscillator strength **(f)** Energy gap **(E_g),** and dipole moment (μ_e), at maximum absorption value without solvent of the newly developed small molecules **C1**, **C2**, **C3** and **C4** and the **R** reference value for **B3LYP** at **Lan2DZ (G) d, p** in gas phase

Molecules	Calculated λ_{max} (eV)	Experimental λ_{max} (eV)	Ex (eV)	*F*	E_g (eV)	Dipole moment (D)
R	519.2	571	2.2632	0.0039	2.71	2.0551
C1	598.53	-	2.167	0.0018	2.57	7.2856
C2	625.41	-	2.097	0.0242	2.53	8.0543
C3	645.53	-	2.043	0.0003	2.54	7.1359
C4	558.37	-	2.319	0.0085	2.69	5.7158

Open circuit voltage (V_{oc})

The open-circuit voltage depends on the individual saturation and the current generated by the light to calculate any of the devices' recombination. It determines the overall amount of current that can be produced from any optical system[32].V_{OC} is actually highest voltage at the level of zero current that can be extracted from any device. To achieve the maximum value of the open-circuit voltage, the HOMO value in the donor material must be higher than the LUMO value in the receiving material. In organic solar cells, donor compounds like polymer such as BDTA etc move their electrons to acceptor compounds for electrical conduction depending on the energy band gap sandwiched between the HOMO of the electron donor compound and the LUMO of the electron acceptor compound also defined as open-circuit voltage (V_{OC}) [33].

Generally, V_{OC} focuses on mutually the saturation current and the light produced current to assist the recombination of the systems. The open circuit voltages can be determined by scale - up the HOMO of the donor and the LUMO of the acceptor species. In order to obtain larger V_{OC}, the LUMO level of the electron acceptor must be high and, in exchange, the HOMO level must be lower level[34] Utilizing electron-donating as well as electron-withdrawing units inside the compound, lower band gap energy is recorded to raise the absorption coefficient, resulting in a rise in V_{OC} as well as light-harvesting capacity. The energy band difference will be minimized if the HOMO and LUMO of the polymer are at higher and lower energy level, accordingly[35, 36].

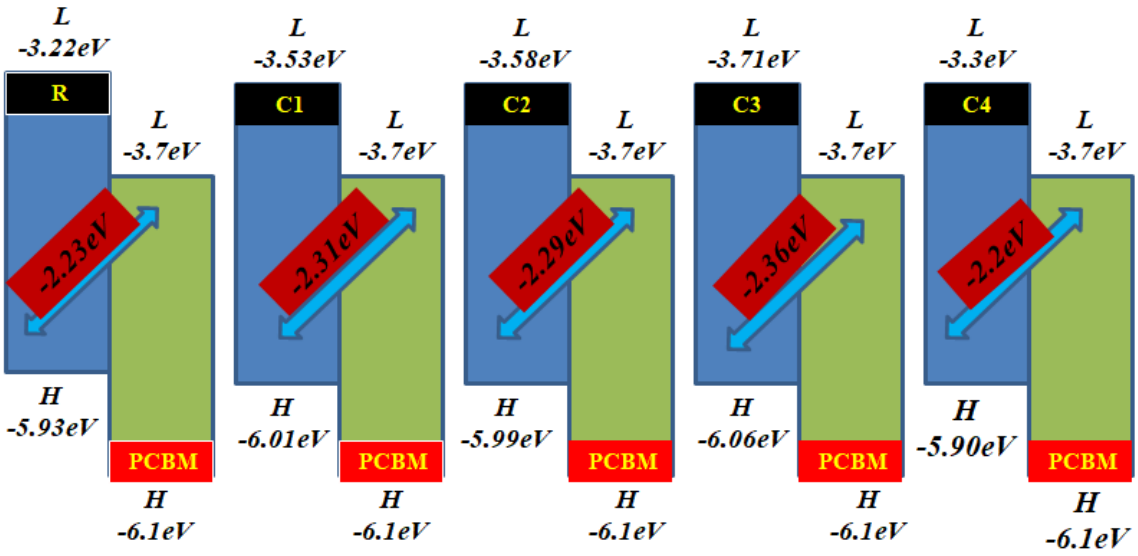

Fig.8. For **PCBM** polymer, Expected open-circuit voltage and design donor molecule (**C1**- **C4**) of the **R**.

Here, we correlated our small molecules constructed by well-known **PCBM** donor polymers to the lowest unoccupied molecular orbitals (LUMOs). Results can be found in Figure 6. The open-circuit voltage measured for **R** concerning **PCBM** is 2.23 eV. **C3** displayed the highest open-circuit voltage value, 2.36 eV, of all molecules.

References

1. Kammen, D.M., *The rise of renewable energy.* Scientific American, 2006. **295**(3): p. 84-93.
2. Green, M.A., *Corrigendum to 'Solar cell efficiency tables (version 46)'[Prog. Photovolt: Res. Appl. 2015; 23: 805–812].* Progress in Photovoltaics: Research and Applications, 2015. **23**(9): p. 1202-1202.
3. Tull, B., *Photovoltaic Cells: Science and Materials.* Columbia University, 2004. **20**(11).
4. Bagher, A.M., *Comparison of organic solar cells and inorganic solar cells.* International Journal of Renewable and Sustainable Energy, 2014. **3**(3): p. 53-58.
5. Perepichka, I.F. and D.F. Perepichka, *Handbook of Thiophene-Based Materials: Applications in Organic Electronics and Photonics, 2 Volume Set*. 2009: John Wiley & Sons.
6. Huang, J., et al., *Boosting organic photovoltaic performance over 11% efficiency with photoconductive fullerene interfacial modifier.* Solar Rrl, 2017. **1**(1): p. 1600008.
7. Brabec, C.J., et al., *Organic photovoltaics: concepts and realization*. Vol. 60. 2003: Springer Science & Business Media.
8. Zhao, F., et al., *Single-junction binary-blend nonfullerene polymer solar cells with 12.1% efficiency.* Advanced Materials, 2017. **29**(18): p. 1700144.
9. Kim, J.Y., et al., *Low band gap poly (thienylene vinylene)/fullerene bulk heterojunction photovoltaic cells.* The Journal of Physical Chemistry C, 2009. **113**(24): p. 10790-10797.
10. Ganesamoorthy, R., G. Sathiyan, and P. Sakthivel, *Fullerene based acceptors for efficient bulk heterojunction organic solar cell applications.* Solar Energy Materials and Solar Cells, 2017. **161**: p. 102-148.
11. Zhou, H., et al., *Donor− acceptor polymers incorporating alkylated dithienylbenzothiadiazole for bulk heterojunction solar cells: pronounced effect of positioning alkyl chains.* Macromolecules, 2010. **43**(2): p. 811-820.
12. Liu, Y., et al., *Spin-coated small molecules for high performance solar cells.* Advanced Energy Materials, 2011. **1**(5): p. 771-775.
13. Sahu, D., et al., *Synthesis and applications of novel low bandgap star-burst molecules containing a triphenylamine core and dialkylated diketopyrrolopyrrole arms for organic photovoltaics.* Journal of Materials Chemistry, 2012. **22**(16): p. 7945-7953.
14. Kimura, M., et al., *Synthesis of multicomponent systems composed of one phthalocyanine and four terpyridine ligands.* Inorganic chemistry, 2001. **40**(18): p. 4775-4779.
15. Liang, D., et al., *Density functional theory calculations of photophysical properties of linear 2, 7-carbazole derivatives as solar cell materials.* Molecular Physics, 2012. **110**(7): p. 369-375.
16. Frisch, M., F. Clemente, and G. Trucks, *Gaussian 09 Rev C. 01 [CP]*. Pittsburgh PA: Gaussian Inc, 2009.
17. Parr, R.G., *W. Yang Density functional theory of atoms and molecules.* O xford University Press, 1989. **1**: p. 989.

18. Yanai, T., D.P. Tew, and N.C. Handy, *A new hybrid exchange–correlation functional using the Coulomb-attenuating method (CAM-B3LYP).* Chemical physics letters, 2004. **393**(1-3): p. 51-57.
19. Adamo, C. and V. Barone, *Exchange functionals with improved long-range behavior and adiabatic connection methods without adjustable parameters: The m PW and m PW1PW models.* The Journal of chemical physics, 1998. **108**(2): p. 664-675.
20. Hertwig, R.H. and W. Koch, *On the parameterization of the local correlation functional. What is Becke-3-LYP?* Chemical Physics Letters, 1997. **268**(5-6): p. 345-351.
21. Chai, J.-D. and M. Head-Gordon, *Long-range corrected hybrid density functionals with damped atom–atom dispersion corrections.* Physical Chemistry Chemical Physics, 2008. **10**(44): p. 6615-6620.
22. Curtiss, L.A., et al., *Extension of Gaussian-2 theory to molecules containing third-row atoms Ga–Kr.* The Journal of Chemical Physics, 1995. **103**(14): p. 6104-6113.
23. Check, C.E., et al., *Addition of polarization and diffuse functions to the LANL2DZ basis set for p-block elements.* The Journal of Physical Chemistry A, 2001. **105**(34): p. 8111-8116.
24. Bjorgaard, J.A., K.A. Velizhanin, and S. Tretiak, *Solvent effects in time-dependent self-consistent field methods. II. Variational formulations and analytical gradients.* The Journal of chemical physics, 2015. **143**(5): p. 054305.
25. Mennucci, B., R. Cammi, and J. Tomasi, *Excited states and solvatochromic shifts within a nonequilibrium solvation approach: A new formulation of the integral equation formalism method at the self-consistent field, configuration interaction, and multiconfiguration self-consistent field level.* The Journal of chemical physics, 1998. **109**(7): p. 2798-2807.
26. González-Rodríguez, D., et al., *Tuning Photoinduced Energy-and Electron-Transfer Events in Subphthalocyanine–Phthalocyanine Dyads.* Chemistry–A European Journal, 2005. **11**(13): p. 3881-3893.
27. Hutchison, G.R., M.A. Ratner, and T.J. Marks, *Intermolecular charge transfer between heterocyclic oligomers. Effects of heteroatom and molecular packing on hopping transport in organic semiconductors.* Journal of the American Chemical Society, 2005. **127**(48): p. 16866-16881.
28. O'boyle, N.M., A.L. Tenderholt, and K.M. Langner, *Cclib: a library for package-independent computational chemistry algorithms.* Journal of computational chemistry, 2008. **29**(5): p. 839-845.
29. Lu, T. and F. Chen, *Multiwfn: a multifunctional wavefunction analyzer.* Journal of computational chemistry, 2012. **33**(5): p. 580-592.
30. Martinelli, N.G., et al., *Influence of structural dynamics on polarization energies in anthracene single crystals.* The Journal of Physical Chemistry C, 2010. **114**(48): p. 20678-20685.
31. Zheng, L., et al., *Where is the electronic oscillator strength? Mapping oscillator strength across molecular absorption spectra.* The Journal of Physical Chemistry A, 2016. **120**(11): p. 1933-1943.
32. Tang, S. and J. Zhang, *Design of donors with broad absorption regions and suitable frontier molecular orbitals to match typical acceptors via substitution on oligo (thienylenevinylene) toward solar cells.* Journal of computational chemistry, 2012. **33**(15): p. 1353-1363.
33. Dennington, R., T. Keith, and J. Millam, *GaussView, version 5.* 2009.
34. Bai, H., et al., *Acceptor–donor–acceptor small molecules based on indacenodithiophene for efficient organic solar cells.* ACS applied materials & interfaces, 2014. **6**(11): p. 8426-8433.
35. Ma, X., et al., *Ternary nonfullerene polymer solar cells with efficiency> 13.7% by integrating the advantages of the materials and two binary cells.* Energy & Environmental Science, 2018. **11**(8): p. 2134-2141.
36. Bibi, S., et al., *Effect of different topological structures (D-π-D and D-π-A-π-D) on the optoelectronic properties of benzo [2, 1-B: 3, 4-Ḃ] dithiophene based donor molecules toward organic solar cells.* Solar Energy, 2019. **186**: p. 311-322.

AUTHORS

First Author – Faheem Abbas, University of Agriculture Faisalabad, Pakistan
Second Author – Tayyaba Nasir, University of Agriculture Faisalabad, Pakistan
Third Author – Muhammad Awais Ahmad, Government College University Faisalabad, Pakistan
Fourth Author – Saira Sehar, Minhaj University Lahore, Pakistan
Fifth Author – Rida Zulfiqar, University of Agriculture Faisalabad, Pakistan
Sixth Author – Muhammad Shaid Iqbal, Government College University Faisalabad, Pakistan
Seventh Author – Muhammad Ishaq, University of Agriculture Faisalabad, Pakistan

Corresponding Author: tayyaba.nasir2726@gmail.com.